Scientific Research Publishing

World Journal of Engineering and Technology, 2025, 13(4), 845-854
https://www.scirp.org/journal/wjet
ISSN Online: 2331-4249
ISSN Print: 2331-4222

Digital Application on the Impact of Terrain on the Threshold Crossing Height Rising

Chunqing Qu[1,2]

[1]Equipment Operation Monitoring Center, East China Regional Air Traffic Management Bureau of Civil Aviation of China, CAAC, Shanghai, China
[2]Digitalization Innovative Laboratory, East China Regional Air Traffic Management Bureau of Civil Aviation of China, CAAC, Shanghai, China
Email: qcq04@163.com

How to cite this paper: Qu, C.Q. (2025) Digital Application on the Impact of Terrain on the Threshold Crossing Height Rising. *World Journal of Engineering and Technology*, **13**, 845-854.
https://doi.org/10.4236/wjet.2025.134053

Received: September 16, 2025
Accepted: October 19, 2025
Published: October 22, 2025

Abstract

The terrain factors have a direct impact on the structure and spatial synthesis of the glide path antenna. Analyzing various terrain factors can effectively control the adjustment effect of Threshold Crossing Height (*TCH*). The *TCH* can be raised by tilting the antenna at a certain angle (ϕ = 0 - 10 degrees). The terrain research will be performed on the Forward Slope (*FSL*), Sideways Slope (*SSL*), and reflector height (h) one by one, and the relationship between these factors will be revealed. Variation of Forward and Sideway Slope (*FSL* = −2˚, −1.5˚, −1˚, −0.5˚, 0˚, +0.5˚, +1˚, +1.5˚, +2˚; *SSL* = −2˚, −1˚, 0˚, +1˚, +2˚) have regular variation in the effect of *TCH* adjustment, while different reflection surface height (h = −2 m, −1.5 m, −1 m, −0.5 m, 0 m, +0.5 m, +1 m, +1.5 m, +2 m) have poor relationship with the effect of adjusting the *TCH*. The increase in *TCH* in complex terrain can be achieved by a smart chart. At the same time, the required tilt angle of the antenna can be inferred directly based on the upward adjustment.

Keywords

Glide Path, Forward Slope, Sideways Slope, Reflector

1. Introduction

The glide slope beacon [1] plays an important role in the Instrument Landing System [2]-[6] (ILS). When the glide slope equipment is used in conjunction with the Distance Measuring Equipment (DME) [7], it can provide vertical guidance for the aircraft and provide continuous distance information, thereby achieving a precise approach. There are three types of glide slope beacons widely used at airports:

null reference glide slope antenna [8], sideband reference glide slope antenna [9], and capture effect glide slope antenna [10]. In flight inspection, Threshold Crossing Height (*TCH*) is an important subject for the glide slope antenna, and it needs to meet the requirement of a range of 15 meters plus 3 meters. The *TCH* cannot be adjusted on the software, mainly by adjusting the antenna. This value can be decreased effectively by moving the lateral offset of the antenna, but the adjustment amount is not large, and the regularity is not strong. Although this parameter can be effectively changed by adjusting the antenna height, the disadvantage is that it affects the Far-Field [11] signal distribution and the glide path angle [12] drifts synchronously. The effective way to adjust the *TCH* is to rotate the antenna. It can not only avoid the deviation of the glide path angle, but also effectively adjust the entrance height regularly. Due to the different Antenna Distribution Unit (ADU) of the three types of antennas mentioned above, the capture effect glide path antenna and the sideband reference glide path antenna can achieve changes in the *TCH* by rotating the upper antenna, while the zero reference glide slope antenna cannot adjust in this way because the signal distribution in the design is too single, and the sideband signal (Side and Bands Only, SBO) is only fed to the upper antenna. In fact, the terrain of each airport varies. Under different terrains, the change in *TCH* varies with the same angle ϕ of antenna rotation. Especially, the height of the reflector in front of the antenna array changes. For example, the growth of grass in a protected area is equivalent to the overall elevation of the ground, or the sinking of local foundations in protected areas causes the overall reduction of the reflector. Taking the capture effect glide path antenna as the research target by rotating the upper antenna, the effect of different terrain factors on the increase of entrance height is analyzed.

2. Methods

2.1. Forward Slope (*FSL*)

When *FSL* exists, the antennas need to be forward offset as well as height adjusted. The height adjustment way is shown in Formula 1. To achieve the target of the antenna being perpendicular to the average forward slope, the antennas shall be set to the forward shift. For an uphill slope, namely $FSL > 0$, keep the upper antenna stationary, and the lower and middle antennas are moved towards the threshold of the runway at a ratio of 2:1, seen in Formulas 2, 3, and 4; the heights of the three antennas increase proportionally, as described in **Figure 1**.

$$h_a = \frac{c}{4f\sin\left(3^\circ - FSL\right)} \tag{1}$$

When $FSL = 0$, h_0 is 4.3 meters, corresponding to a frequency of the transmitter is 333.35 MHz. Whereas the direction from the GP tower to the runway threshold, the value is positive.

$$sft_u = \left(h_u - h_u\right)\sin\left(FSL\right) = 0 \tag{2}$$

$$sft_m = (h_u - h_m)\sin(FSL) = h_a \sin(FSL) \quad (3)$$

$$sft_d = (h_u - h_d)\sin(FSL) = 2h_a \sin(FSL) \quad (4)$$

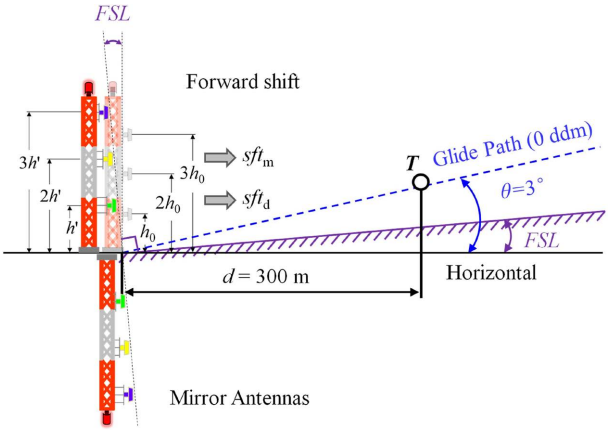

Figure 1. (Color online) Forward Slope (*FSL*) and antenna forward shift. The three antennas should be aligned along a straight line, which shall be perpendicular to the average forward slope. If the *FSL* is rising, the lower antenna shall be forward compared to the middle antenna and the upper antenna. At the same time, the antenna's height should also be adjusted synchronously. In the case of *FSL* = 0˚, the three antennas focus on the same point in a top view.

And for a downhill slope, that is to say, *FSL* < 0, keep the lower antenna stationary, and the upper and middle antennas are moved towards the threshold of the runway at a ratio of 2:1. To ensure that the synthesized signal remains at a 3˚ elevation angle, the heights of the three antennas decrease proportionally.

2.2. Sideways Slope (*SSL*)

When *SSL* is present, the antennas need to be laterally offset. The lateral offset of the antenna is related to two factors: one is to calibrate the phase difference from antennas to the surface of the center line of the runway, and the second is to calibrate the terrain changes caused by the sideways slope. For the first scenario, the upper and lower antennas are offset in the opposite direction, with a bias of 5:3. The movement is determined by the antenna height *h* and *SSL*, and the middle antenna remains stationary, as shown at the bottom of Figure 2. For the second scenario, the three antennas are perpendicular to *SSL*, while the middle antenna remains stationary, and the upper and lower antennas are offset in the opposite direction, with a bias of 1:1. The movement is determined by the antenna height *h* and the lateral distance *l*, as seen at the top of Figure 2.

For antenna phase difference calibration, the centerline of the runway is on the horizontal plane. When considering the sideways slope situation, the calibration point of the runway centerline is located on the slope surface. The final combined offset effect of the ground antennas and mirror antennas is presented in Figure 3, which can be regarded as a section of arc, consisting of six antennas with the surface of the runway centerline as the center. For the setting of bias, keep the middle

antenna stationary for ease of operation, and only move the upper and lower antennas.

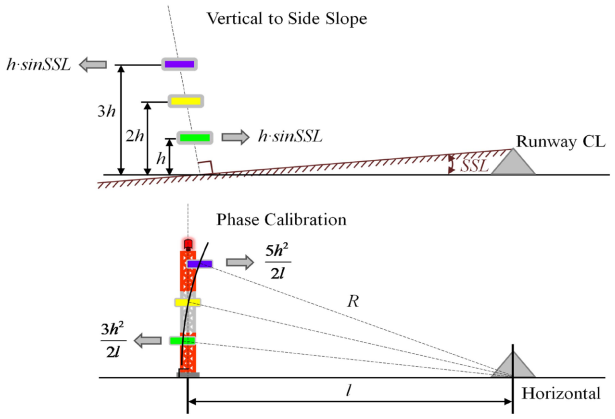

Figure 2. (Color online) Lateral antenna offset for Sideways Slope (*SSL*) and phase difference calibration. The antennas shall be perpendicular to the average sideways slope. Besides, to calibrate the phase difference from antennas to the surface of the center line of the runway, the upper antenna is closer to the runway than the middle antenna, and the middle antenna shall be closer to the runway than the lower antenna, accompanied by an additional movement.

$$off_u = -\frac{5h_a^2}{2l} + h_a \sin(SSL) \tag{5}$$

$$off_d = \frac{3h_a^2}{2l} - h_a \sin(SSL) \tag{6}$$

The bias of the upper and lower antennas is shown in Formulas 5 and 6. Whereas the direction close to the runway is negative, and the direction far away from the runway to GP, the value is positive. It is worth noting that if *FSL* exists, the antenna height is converted to h_a, as introduced in Formula 1. In fact, the three mirror antennas also generated lateral bias, as listed in Figure 3.

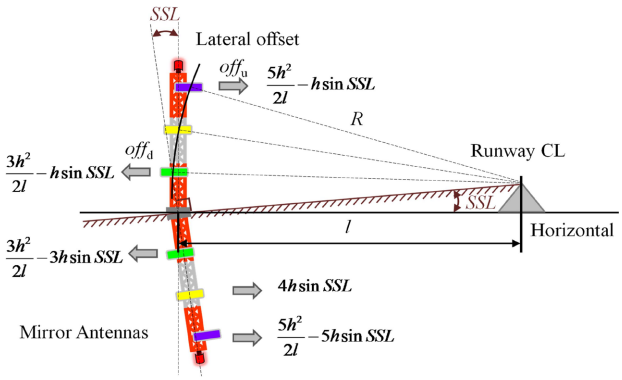

Figure 3. (Color online) The final movement result of lateral offset for the *SSL* and phase difference calibration work together.

2.3. Reflection Plane Rising or Sinking

When a huge amount of snow heaps up, it can cause the reflective surface to rise.

In addition, the growth of wild grass in front of the antenna array can also cause the reflective surface to rise. The factors of raising the height of reflective surfaces will cause the antenna's height to decrease. On the contrary, ground foundation subsidence in front of the antenna array will increase the height of the antenna. Assuming that the height of the reflective surface in front of the antenna array varies as a whole, the height variation of the ground antenna and the mirror antenna is shown in Figure 4. The height of the upper, middle, and lower antennas varies as a whole, and the height ratio is no longer 3:2:1.

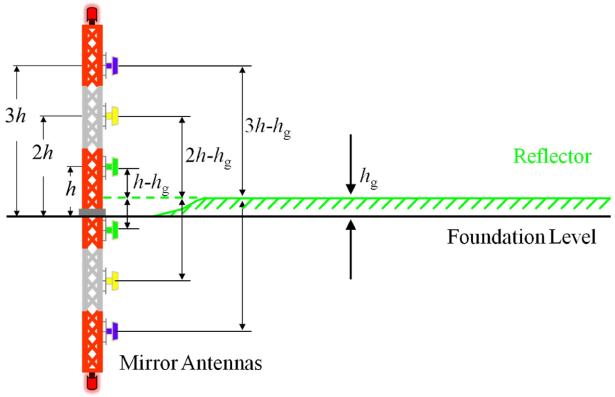

Figure 4. (Color online) The height variation of the reflector (h_g) causes a change in the height of the ground and mirror antennas. To distinguish antenna height, the change in reflector height is represented by h_g. Once the height of the reflector is raised by h_g, the height of the ground antennas would be reduced by h_g, and the height of the mirror antennas would be reduced by twice h_g.

The impact of the three terrain factors on the height and offset of the antennas is summarized in Table 1. h_g only affects the height of the antennas, *FSL* has an impact on the antenna height, and the lateral and forward offset of the antennas are adjusted accordingly. *SSL* only affects the lateral offset of antennas and has no effect on the antenna height and forward offset. In summary, *FSL* has the greatest impact on antenna position.

Table 1. The influence of terrain on antenna position.

	h_g	*FSL*	*SSL*
h_a	√	√	×
sft	×	√	×
off	×	√	√

2.4. Method to Achieve *TCH* Rising

The 3D model is established by MATLAB, the frequency is taken as 333.35 MHz, the corresponding wavelength is 0.9 m. The drawback distance is 300 m, and the lateral distance is 120 m. During the flight of approach, the pilot continuously tracked the zero points position of DDM on the glide slope to obtain the *TCH*.

According to the flight verification rules, the sampling interval for the *TCH* is the area between 1830 meters and 300 meters from the runway threshold. The data of the zero points of DDM tracked in this region is fitted, and the fitted curve is extended to the corresponding value at the runway threshold, which value is the *TCH*. Antenna rotation is applied to adjust *TCH*, and it can be precisely set. When the upper antenna is rotated horizontally towards the runway, ϕ is defined as positive, and consequently, the *TCH* is rising. The DDM curves from 1830 to 300 meters with $\phi = 10^{\circ}$ are exhibited in Figure 5. At the position of 1830 m with Far-Field (FF) [13], the distribution of DDM curves is relatively dense, and the 0 ddm position is less than 3 degrees. Generally speaking, the distance is 100 times the height of the upper antenna, namely, 1300 meters away from the antenna is the far-field, and the radiation path from the upper, middle, and lower antennas to the receiving point of the far-field can be considered as parallel. When approaching the runway threshold, the interval at the same distance along the DDM curve distribution increases, and at a position of 300 m, the angle of the zero point exceeds 3.2 degrees. The blue dots represent the zero point of each DDM curve, as shown in the insert of Figure 5.

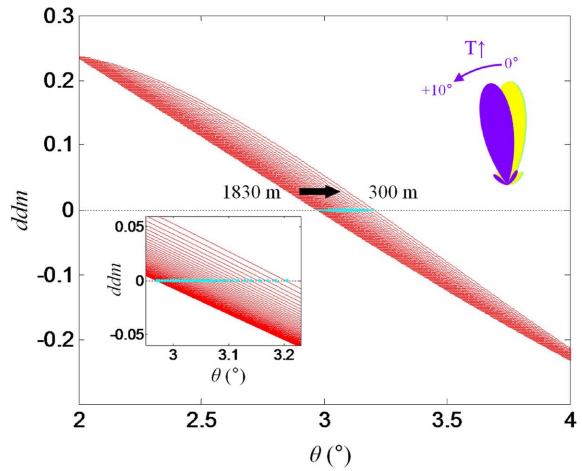

Figure 5. (Color online) The DDM patterns from 1830 m to 300 m to the runway threshold of the upper antenna rotation in horizontal. The selection of the interval is 30 m. When the upper antenna rotates to the runway, the *TCH* will be raised. The larger the rotation angle ϕ, the higher the *TCH* rises.

2.5. Method to Achieve the Final Increment of *TCH*

There are three factors: F1 is a two-dimensional matrix that is the correlation coefficient between *FSL* and *h*, F2 is the coefficient of the factor of *h*, F3 is the coefficient of the rotation angle ϕ, and the product of the three coefficients is the final increment of *TCH* (ΔT) after antenna rotation in different terrains.

3. Results and Discussion

Antenna rotation in three different terrain conditions is applied to raise the ΔT, and a digital table is summarized for conversion based on the distribution char-

acteristics of the various terrains.

3.1. Parameters Responding

Considering the half-width with −3 dB power (0.707 amplitude) of Kathrein lobe is 12.5˚. Excessive rotation angle can lead to insufficient coverage. So, the rotation angle ϕ in this study is restricted to ±10˚ to ensure that the typical radiation power of 20 W can meet the glide path coverage requirements [14] with 18.5 km within ±8˚ in horizontal.

The ΔT patterns of different terrain conditions are shown in Figure 6. There is no special variation for the *SSL* response. The response of ΔT to *FSL* is very strong and regular. For every certain rotation angle ϕ, the interval of ΔT with different *FSL* is almost identical, as marked in the middle of Figure 6. The response of ΔT to h is also evident, the intervals of ΔT increasing monotonically with h, and the larger h, the larger the ΔT interval.

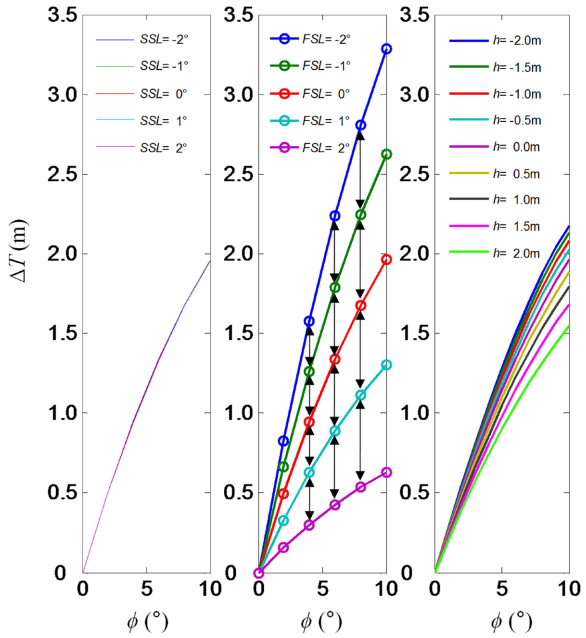

Figure 6. (Color online) ΔT corresponding to ϕ with a series of *SSL*, *FSL*, and the height variation of reflector h.

3.2. Method for Predicting

Through the correlation between three terrain factors, the method to calculate between the rotating angle (ϕ) and the variation of T (ΔT) is refined. It can be obtained accurately by table look-up.

3.2.1. The Impact of *SSL* on the Other Terrain Factors

The interactive impact of *FSL* on *SSL* is negligible. While the interaction of h and *SSL* exists. In extreme conditions, the calculation errors should be studied. In the case of $FSL = -2^{\circ}$, $h = -2$ m, the data difference is −0.09 m for $SSL = -2^{\circ}$, and 0.07 m for $SSL = 2^{\circ}$. In the case of $FSL = -2^{\circ}$, $h = 1$ m, the data difference is 0.06 m for

SSL = −2˚, and 0.07 m for *SSL* = 2˚. All in all, the variation of *SSL* will cause a final error within ±0.1 m. According to the calculation, the smaller the absolute value of *SSL*, the smaller the error. Therefore, when SSL is between −2˚ and +2˚, the impact of error on the results is smaller. Also, the negligible difference of *SSL* can be found in the left of Figure 6. The International Civil Aviation Organization (ICAO) limits the range of T to 15 m +3 m. A few centimeters have little impact on the adjustment of *TCH*. So, the calculation error caused by the factor of *SSL* can be ignored in the following discussion.

3.2.2. Accurate Calculation from Table

Through the correlation calculation and analysis of *h*, *FSL*, and ϕ, normalized calculation and data deviation analysis are summarized in Table 2, which consists of three parts. The first part is the correlation coefficient between *FSL* and *h*, the second part is only related to the *h* factor, and the third part is the rotation coefficient. F1 and F2 are just coefficients, and F3 corresponds to ΔT in meters. For terrains with different *FSL* and reflector heights, find the corresponding coefficients F1 and F2 for *FSL* and *h* values, and then find the corresponding coefficient F3 based on the rotation angle ϕ. Multiply the three to obtain the increment of *TCH*, that is, the terminal ΔT. There are two cases exhibited.

In case of *FSL* = −0.5˚, *h* = 1.5 m, ϕ = 6˚, ΔT = 1.199*0.856*1.34 = 1.375 m. The value of ΔT obtained from the 3D model is 1.3619 m, and the error is just 0.96%.

In case of *FSL* = 1.5˚, *h* = −1 m, ϕ = 10˚, ΔT = 0.517*1.063*1.965 = 1.08 m. The value of ΔT calculated from the established GP model is 1.0928 m, and the error is 1.2%.

Table 2. Coefficients of terrain factors.

	h (m)	−2.0 m	−1.5 m	−1.0 m	−0.5 m	0.0 m	0.5 m	1.0 m	1.5 m	2.0 m
	FSL (˚)									
F1	−2.0˚	1.442	1.495	1.554	1.612	1.671	1.742	1.790	1.830	1.801
	−1.5˚	1.340	1.378	1.421	1.462	1.505	1.555	1.585	1.614	1.594
	−1.0˚	1.238	1.261	1.288	1.312	1.339	1.367	1.380	1.397	1.386
	−0.5˚	1.119	1.131	1.144	1.156	1.170	1.184	1.190	1.199	1.193
	0.0˚	1.000	1.000	1.000	1.000	1.000	1.000	1.000	1.000	1.000
	0.5˚	0.860	0.852	0.844	0.837	0.831	0.827	0.821	0.819	0.815
	1.0˚	0.719	0.704	0.688	0.675	0.663	0.654	0.643	0.638	0.630
	1.5˚	0.549	0.533	0.517	0.502	0.491	0.484	0.475	0.468	0.465
	2.0˚	0.378	0.362	0.345	0.329	0.319	0.314	0.307	0.299	0.299
	h (m)	−2.0 m	−1.5 m	−1.0 m	−0.5 m	0.0 m	0.5 m	1.0 m	1.5 m	2.0 m
F2	*h* factor	1.112	1.089	1.063	1.036	1.000	0.957	0.912	0.856	0.789
	ϕ (˚)	2	3	4	5	6	7	8	9	10
F3	ΔT (m)	0.496	0.726	0.945	1.149	1.340	1.518	1.679	1.833	1.965

3.2.3. Reverse Estimation by Interpolation Method

It can be calculated that ΔT from ϕ in a variety of terrains. However, what is more worthy of note is to estimate ϕ from ΔT. In practice, ΔT is the preset value, while the expected value ϕ is what we really need. While the needed rotating angle could not be calculated directly, it can be achieved by speculating in reverse estimation. The rotating angle ϕ can be reverse calculated by the interpolation method.

For example, in case of $FSL = -0.5^\circ$, $h = 1.5$ m and $\Delta T = 2$ m, it can be calculated that F3 = ΔT/F1/F2 = 2/1.199/0.856 = 1.949 m. It can be seen that the ϕ is between 9˚ and 10˚, which can be obtained by the interpolation method. $\phi = (1.949 - 1.833)/(1.965 - 1.833) + 9 = 9.88^\circ$. On the contrary, substituting $\phi = 9.88^\circ$ into the calculation yields $\Delta T = 1.9956$ m; the error is 0.22%.

Example two, in case of $FSL = 1.5^\circ$, $h = -1$ m, $\Delta T = 0.5$ m, then F3 = ΔT/F1/F2 = 0.5/0.517/1.063 = 0.91 m. It can be seen that the ϕ is between 3˚ and 4˚, $\phi = (0.91 - 0.726)/(0.945 - 0.726) + 3 = 3.84^\circ$. Substituting $\phi = 3.84^\circ$ into the calculation yields $\Delta T = 0.5083$ m; the error is 1.7%.

4. Summary/Conclusion

A special method of adjustment of *TCH* by antenna tilt is investigated concerning a series of factors of the terrain. *TCH* can be raised freely and accurately by the rotation of the upper antenna. The regularity of variation related to Sideways Slope (*SSL*), Forward Slope (*FSL*), and the variation height of the reflector (h) is revealed digitally and intensively. The adjustment effect of ΔT decreases by 33% for every degree increase in *FSL*. The impact of the sideways slope on the adjustment effect can be ignored. The smaller the h, the better the effect adjustment, resulting in a monotonic change. The calculation results between the rotating angle (ϕ) and the variation of *TCH* (ΔT) can be obtained accurately by table look-up. However, what is more worthy of attention is the expected value ϕ. This is what we really need. It can be achieved by speculating in reverse. The research worker can be applied in a variety of airports with a wide range of fields. In further work, to create a more intelligent method, more complex terrain factors, such as curved reflective surfaces, would be taken into account.

Conflicts of Interest

The author declares no conflicts of interest regarding the publication of this paper.

References

[1] Xu, J., Ye, J., Liang, F., Li, Y. and Lin, H. (2021) Simulation Analysis and Research on the Influence of Buildings on a Glide Path Antenna. 2021 *International Conference on Computer Technology and Media Convergence Design* (*CTMCD*), Sanya, 23-25 April 2021, 63-66. https://doi.org/10.1109/ctmcd53128.2021.00022

[2] Kwasiborska, A., Grabowski, M., Sedláčková, A.N. and Novák, A. (2023) The Influence of Visibility on the Opportunity to Perform Flight Operations with Various Categories of the Instrument Landing System. *Sensors*, **23**, Article No. 7953. https://doi.org/10.3390/s23187953

[3] Novák, A., Havel, K. and Janovec, M. (2017) Measuring and Testing the Instrument Landing System at the Airport Zilina. *Transportation Research Procedia*, **28**, 117-126. https://doi.org/10.1016/j.trpro.2017.12.176

[4] Sun, J. (2024) Specification for Instrument Landing System. *Exploration of Educational Management*, **2**, 107-111.

[5] Geise, R., Neubauer, B., Weiß, A. and Akar, A. (2024) On the Imaging of Large Antenna Array Navigation Systems: IWAC2022 Special Issue: Selected Papers from the 2022 International Workshop on ATM/CNS. *Transactions of the Japan Society for Aeronautical and Space Sciences*, **67**, 119-126. https://doi.org/10.2322/tjsass.67.119

[6] Sun, Y.C., Zhu, W.S. and Pucuo, W. (2023) The Necessity of Flight Calibration Temperature Correction of High Plateau Airport Instrument Landing System. *Academic Journal of Engineering and Technology Science*, **6**, 63-66.

[7] Abd-Elaty, E., Zekry, A., El-Agooz, S. and Helaly, A.M. (2022) Underlay Spectrum Sharing with L-Band Distance Measuring Equipment for Aeronautical Communications. *Wireless Personal Communications*, **128**, 2363-2377. https://doi.org/10.1007/s11277-022-10045-0

[8] Normarc (2015) Normarc 3543 Null Reference Glide Path Antenna System Instruction Manual. Oslo Norway.

[9] Normarc (2015) Normarc 3544 Sideband Reference Glide Path Antenna System Instruction Manual. Oslo Norway.

[10] Normarc (2016) Normarc 3545 M-Array Glide Path Antenna System Instruction Manual. Oslo Norway.

[11] Qu, C. (2018) Brief Introduction of a New Kind of Glide Path Antenna. *Open Journal of Antennas and Propagation*, **6**, 60-72. https://doi.org/10.4236/ojapr.2018.63006

[12] Normarc (2018) Normarc7000B Training Manual. Normarc, 23-24.

[13] Qu, C.Q. (2015) Research on Signal of Field Monitor of 7220A Localizer Beacon Subsystem of ILS. *Open Journal of Antennas and Propagation*, **3**, 37-50. https://doi.org/10.4236/ojapr.2015.34005

[14] International Civil Aviation Organization (2006) Annex 10, Aeronautical Telecommunications, Vol. I, 3.1.5.3.1. International Civil Aviation Organization (ICAO).